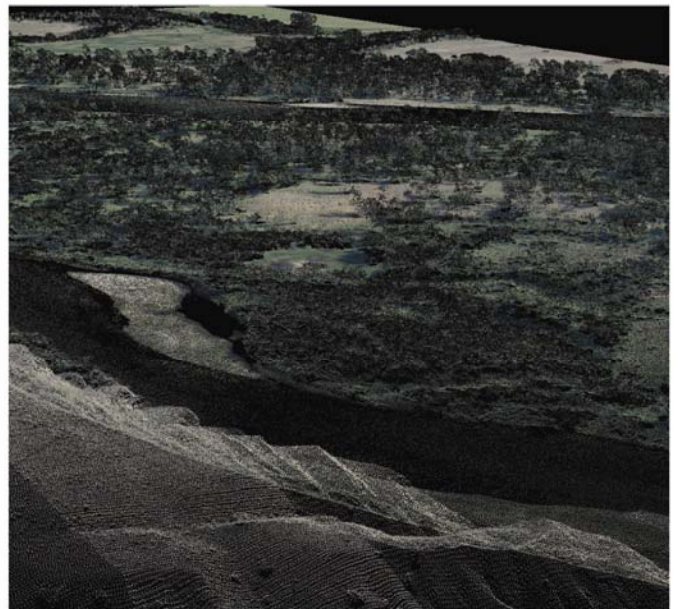


LIDAR REMOTE SENSING & BATHYMETRY

BROADWATER • MONTANA

(DELIVERY - 12/17/2010)



PBS & J INC. • 3810 Valley Commons Drive, Suite 4 - Bozeman, MT 59718

 WATERSHED SCIENCES • 517 SW 2nd Street, Suite 400 - Corvallis, OR 97333

LIDAR REMOTE SENSING DATA COLLECTION: BROADWATER, MT

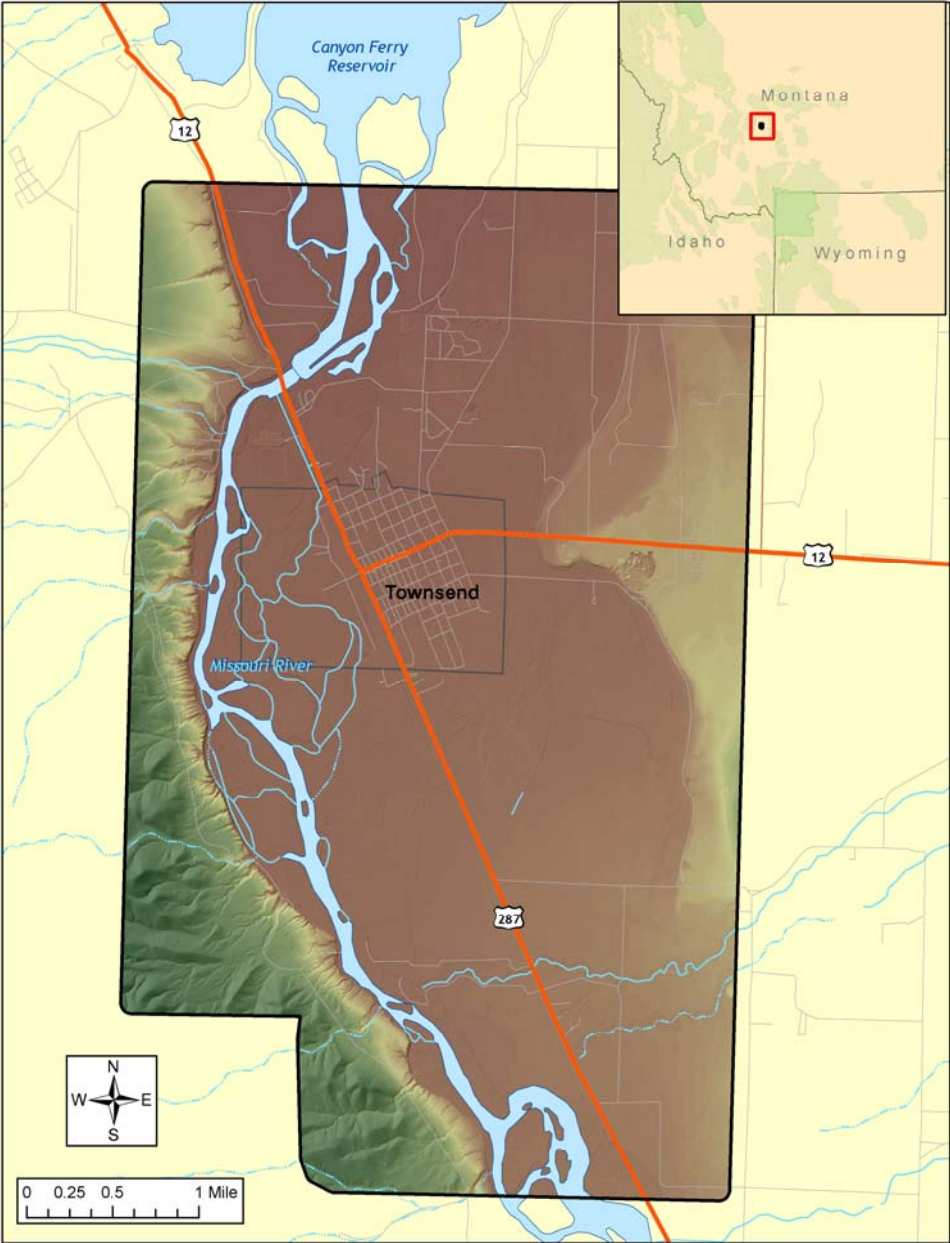
TABLE OF CONTENTS

1. Overview	1
2. Acquisition	2
2.1 Airborne Survey - Instrumentation and Methods	2
2.2 Ground Survey - Instrumentation and Methods	3
2.2.1 Instrumentation	3
2.2.2 Monumentation	3
2.2.3 Methodology	4
3. LiDAR Data Processing	7
3.1 Applications and Work Flow Overview	7
3.2 Aircraft Kinematic GPS and IMU Data	7
3.3 Laser Point Processing	8
3.4 Contour Development	9
4. LiDAR Accuracy Assessment	10
4.1 Laser Noise and Relative Accuracy	10
4.2 Absolute Accuracy	11
5. Study Area Results	11
5.1 Data Summary	11
5.2 Data Density/Resolution	12
5.3 Relative Accuracy Calibration Results	16
5.4 Absolute Accuracy	17
5.5 Accuracy per Land Cover	18
6. Bathymetric Survey	20
6.1 Overview	20
6.2 Bathymetric Survey - Instrumentation and Methods	22
6.3 Bathymetric Data Processing	22
6.4 Bathymetric Accuracy Assessment	23
7. Combined Elevation Model	24
7.1 Bathymetric Processing	25
7.2 Terrestrial LiDAR Extraction	25
7.3 Combined Elevation Model	25
8. Projection/Datum and Units	27
9. Deliverables	27
10. Selected Images	28
11. Glossary	31
12. Citations	32
Appendix A	33

1. Overview

Watershed Sciences, Inc. (WS) collected Light Detection and Ranging (LiDAR) data for Broadwater, MT on October 28th, 2010. Bathymetric data was acquired for a portion of the Missouri River by Solmar Hydro from November 17th to 19th, 2010. This report documents the data acquisition, processing methods, accuracy assessment, and deliverables for the 11,929 acre area of interest (AOI). The requested area was expanded to include a 100m buffer to ensure complete coverage and adequate point densities around survey area boundaries resulting in a total of 12,666 acres of data.

Figure 1. Broadwater, MT area of interest



2. Acquisition

2.1 Airborne Survey - Instrumentation and Methods

The LiDAR survey utilized a Leica ALS60 sensor in a Cessna Caravan 208B. The ALS60 sensor operates with Automatic Gain Control (AGC) for intensity correction. The Leica system was set to acquire $\geq 105,900$ laser pulses per second (i.e., 105.9 kHz pulse rate) and flown at 900 meters above ground level (AGL), capturing a scan angle of $\pm 14^\circ$ from nadir. With these flight parameters, the laser swath width is $\sim 450\text{m}$ and the laser pulse footprint is $\sim 21\text{cm}$. These settings were developed to yield points with an average native pulse density of ≥ 8 pulses per square meter over terrestrial surfaces. It is not uncommon for some types of surfaces (e.g. dense vegetation or water) to return fewer pulses than the laser originally emitted. These discrepancies between 'native' and 'delivered' density will vary depending on terrain, land cover, and the prevalence of water bodies.



The Cessna Caravan is a stable platform, ideal for flying slow and low for high density projects. A Leica ALS50 sensor head installed in the Caravan is shown on the left.

All areas were surveyed with an opposing flight line side-lap of $\geq 50\%$ ($\geq 100\%$ overlap) to reduce laser shadowing and increase surface laser painting. The Leica laser systems allow up to four range measurements (returns) per pulse, and all discernable laser returns were processed for the output dataset.

To accurately solve for laser point position (geographic coordinates x, y, z), the positional coordinates of the airborne sensor and the attitude of the aircraft were recorded continuously throughout the LiDAR data collection mission. Aircraft position was measured twice per second (2 Hz) by an onboard differential GPS unit. Aircraft attitude was measured 200 times per second (200 Hz) as pitch, roll and yaw (heading) from an onboard inertial measurement unit (IMU). To allow for post-processing correction and calibration, aircraft/sensor position and attitude data are indexed by GPS time.

2.2 Ground Survey - Instrumentation and Methods

During the LiDAR survey, static (1 Hz recording frequency) ground surveys were conducted over set monuments. Monument coordinates are provided in **Table 1** and shown in **Figure 2**. After the airborne survey, the static GPS data are processed using triangulation with Continuously Operating Reference Stations (CORS) and checked using the Online Positioning User Service (OPUS¹) to quantify daily variance. Multiple sessions are processed over the same monument to confirm antenna height measurements and reported position accuracy.

Indexed by time, these GPS data are used to correct the continuous onboard measurements of aircraft position recorded throughout the mission. Control monuments were located within 13 nautical miles of the survey area.



2.2.1 Instrumentation

For this delivery area, a Trimble GPS receiver model R7 with Zephyr Geodetic antenna with ground plane was deployed for all static control. A Trimble model R8 GNSS unit was used for collecting check points using real time kinematic (RTK) survey techniques. For RTK data, the collector begins recording after remaining stationary for 5 seconds then calculating the pseudo range position from at least three epochs with the relative error under 1.5cm horizontal and 2cm vertical. All GPS measurements are made with dual frequency L1-L2 receivers with carrier-phase correction.

2.2.2 Monumentation



Watershed Sciences was able to occupy one NGS monument and established a second monument for the area of interest. The Watershed Sciences' monumentation was done with 5/8" x 30" rebar topped with a plastic cap marked with the project ID and technicians initials.

¹ Online Positioning User Service (OPUS) is run by the National Geodetic Survey to process corrected monument positions.

Table 1. Base Station control coordinates for Broadwater, MT AOI

Base Station ID	Datum: NAD83 (CORS96)		GRS80
	Latitude	Longitude	Ellipsoid Z (meters)
BWTR_01	46° 20' 01.76007	111° 31' 37.32099	1149.592
RW0582	46° 18' 33.94917	111° 30' 52.81079	1155.608

2.2.3 Methodology



Trimble GPS survey equipment configured for RTK collection

Each aircraft is assigned a ground crew member with two Trimble R7 receivers and an R8 receiver. The ground crew vehicles are equipped with standard field survey supplies and equipment including safety materials. All control monuments are observed for a minimum of two survey sessions lasting no fewer than 6 hours. At the beginning of every session the tripod and antenna are reset, resulting in two independent instrument heights and data files. Data is collected at a rate of 1Hz using a 10 degree mask on the antenna.

The ground crew uploads the GPS data to our FTP site on a daily basis to be returned to the office for Professional Land Surveyor (PLS) oversight, QA/QC review and processing. OPUS processing triangulates the monument position using 3 CORS stations resulting in a fully adjusted position. After multiple days of data have been collected at each monument, accuracy and error ellipses are calculated from the OPUS reports. This information leads to a rating of the monument based on FGDC-STD-007.2-1998² Part 2 table 2.1 at the 95% confidence level. When a statistical stable position is found CORPSCON³ 6.0.1

software is used to convert the UTM positions to geodetic positions. This geodetic position is used for processing the LiDAR data.

RTK and aircraft mounted GPS measurements are made during periods with PDOP⁴ less than or equal to 3.0 and with at least 6 satellites in view of both a stationary reference receiver and the roving receiver. Static GPS data collected in a continuous session average the high PDOP into the final solution in the method used by CORS stations. RTK positions are collected on bare earth locations such as paved, gravel or stable dirt roads, and other locations where the

² Federal Geographic Data Committee Draft Geospatial Positioning Accuracy Standards

³ U.S. Army Corps of Engineers, Engineer Research and Development Center Topographic Engineering Center software

⁴PDOP: Point Dilution of Precision is a measure of satellite geometry, the smaller the number the better the geometry between the point and the satellites.

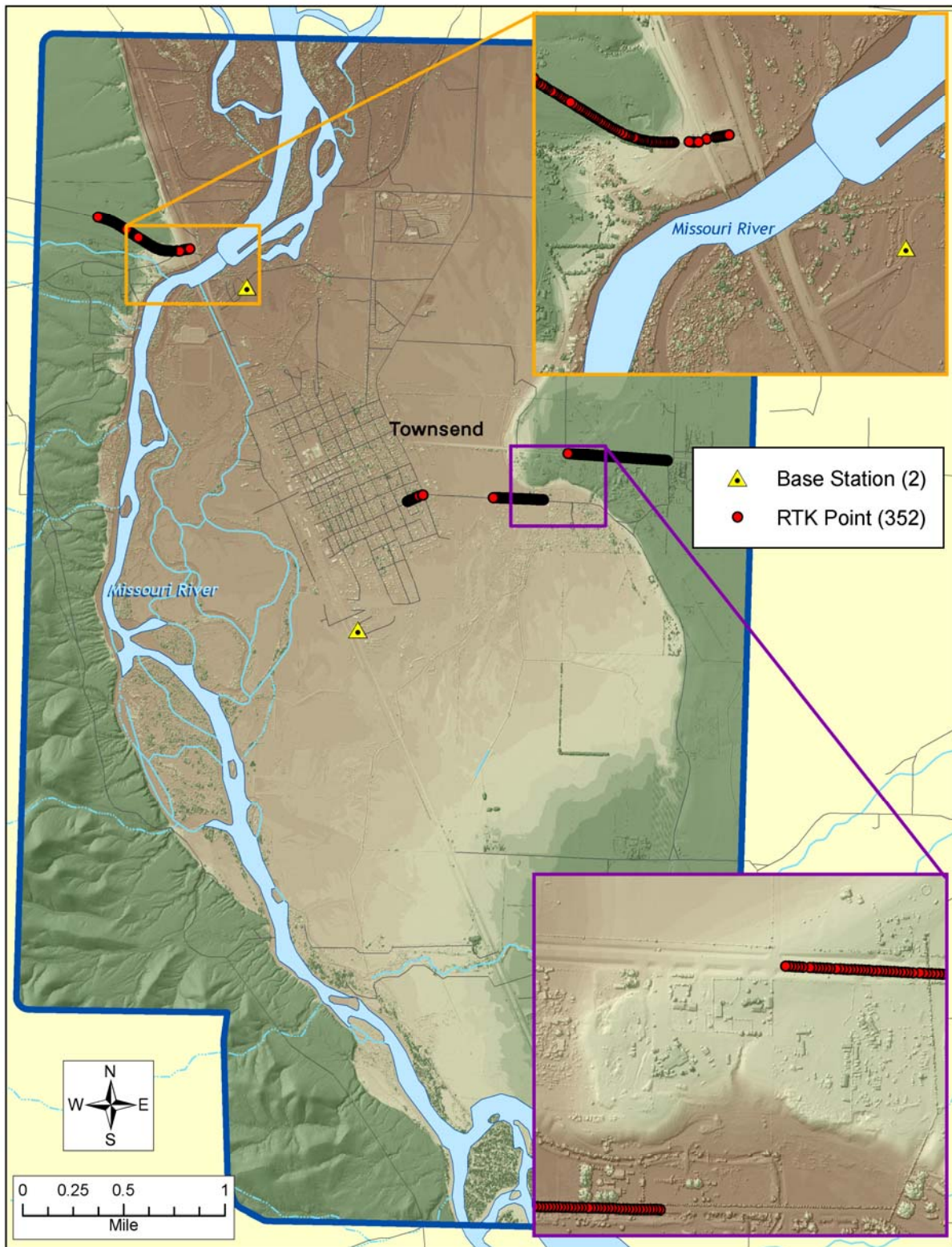
LiDAR Data Acquisition and Processing: Broadwater, MT

ground is clearly visible (and is likely to remain visible) from the sky during the data acquisition and RTK measurement period(s).

In order to facilitate comparisons with LiDAR measurements, RTK measurements are not taken on highly reflective surfaces such as center line stripes or lane markings on roads. RTK points were taken no closer than one meter to any nearby terrain breaks such as road edges or drop offs.



Figure 2. RTK check point and control monument locations used in Broadwater AOI



3. LiDAR Data Processing

3.1 Applications and Work Flow Overview

1. Resolved kinematic corrections for aircraft position data using kinematic aircraft GPS and static ground GPS data.
Software: Waypoint GPS v.8.10, Trimble Geomatics Office v.1.62
2. Developed a smoothed best estimate of trajectory (SBET) file that blends post-processed aircraft position with attitude data. Sensor head position and attitude were calculated throughout the survey. The SBET data were used extensively for laser point processing.
Software: IPAS v.1.35
3. Calculated laser point position by associating SBET position to each laser point return time, scan angle, intensity, etc. Created raw laser point cloud data for the entire survey in *.las (ASPRS v. 1.2) format.
Software: ALS Post Processing Software v.2.70
4. Imported raw laser points into manageable blocks (less than 500 MB) to perform manual relative accuracy calibration and filter for pits/birds. Ground points were then classified for individual flight lines (to be used for relative accuracy testing and calibration).
Software: TerraScan v.10.009
5. Using ground classified points per each flight line, the relative accuracy was tested. Automated line-to-line calibrations were then performed for system attitude parameters (pitch, roll, heading), mirror flex (scale) and GPS/IMU drift. Calibrations were performed on ground classified points from paired flight lines. Every flight line was used for relative accuracy calibration.
Software: TerraMatch v.10.006
6. Position and attitude data were imported. Resulting data were classified as ground and non-ground points. Statistical absolute accuracy was assessed via direct comparisons of ground classified points to ground RTK survey data. Data were then converted to orthometric elevations (NAVD88) by applying a Geoid09 correction.
Software: TerraScan v.10.009, TerraModeler v.10.004
7. Bare Earth models were created as a triangulated surface and exported as ArcInfo ASCII grids at a 3-foot pixel resolution. Highest Hit models were created for any class at 3-foot grid spacing and exported as ArcInfo ASCII grids.
Software: TerraScan v.10.009, ArcMap v. 9.3.1, TerraModeler v.10.004

3.2 Aircraft Kinematic GPS and IMU Data

LiDAR survey datasets were referenced to the 1 Hz static ground GPS data collected over pre-surveyed monuments with known coordinates. While surveying, the aircraft collected 2 Hz kinematic GPS data, and the onboard inertial measurement unit (IMU) collected 200 Hz aircraft attitude data. Waypoint GPS v.8.10 was used to process the kinematic corrections for the aircraft. The static and kinematic GPS data were then post-processed after the survey to obtain an accurate GPS solution and aircraft positions. IPAS v.1.35 was used to develop a trajectory file that includes corrected aircraft position and attitude information. The

LiDAR Data Acquisition and Processing: Broadwater, MT

trajectory data for the entire flight survey session were incorporated into a final smoothed best estimated trajectory (SBET) file that contains accurate and continuous aircraft positions and attitudes.

3.3 Laser Point Processing

Laser point coordinates were computed using the IPAS and ALS Post Processor software suites based on independent data from the LiDAR system (pulse time, scan angle), and aircraft trajectory data (SBET). Laser point returns (first through fourth) were assigned an associated (x, y, z) coordinate along with unique intensity values (0-255). The data were output into large LAS v. 1.2 files with each point maintaining the corresponding scan angle, return number (echo), intensity, and x, y, z (easting, northing, and elevation) information.

These initial laser point files were too large for subsequent processing. To facilitate laser point processing, bins (polygons) were created to divide the dataset into manageable sizes (< 500 MB). Flightlines and LiDAR data were then reviewed to ensure complete coverage of the survey area and positional accuracy of the laser points.

Laser point data were imported into processing bins in TerraScan, and manual calibration was performed to assess the system offsets for pitch, roll, heading and scale (mirror flex). Using a geometric relationship developed by Watershed Sciences, each of these offsets was resolved and corrected if necessary.

LiDAR points were then filtered for noise, pits (artificial low points), and birds (true birds as well as erroneously high points) by screening for absolute elevation limits, isolated points and height above ground. Each bin was then manually inspected for remaining pits and birds and spurious points were removed. In a bin containing approximately 7.5-9.0 million points, an average of 50-100 points are typically found to be artificially low or high. Common sources of non-terrestrial returns are clouds, birds, vapor, haze, decks, brush piles, etc.

Internal calibration was refined using TerraMatch. Points from overlapping lines were tested for internal consistency and final adjustments were made for system misalignments (i.e., pitch, roll, heading offsets and scale). Automated sensor attitude and scale corrections yielded 3-5 cm improvements in the relative accuracy. Once system misalignments were corrected, vertical GPS drift was then resolved and removed per flight line, yielding a slight improvement (<1 cm) in relative accuracy.

The TerraScan software suite is designed specifically for classifying near-ground points (Soininen, 2004). The processing sequence began by 'removing' all points that were not 'near' the earth based on geometric constraints used to evaluate multi-return points. The resulting bare earth (ground) model was visually



inspected and additional ground point modeling was performed in site-specific areas to improve ground detail. This manual editing of ground often occurs in areas with known ground modeling deficiencies, such as: bedrock outcrops, cliffs, deeply incised stream banks, and dense vegetation. In some cases, automated ground point classification erroneously included known vegetation (i.e., understory, low/dense shrubs, etc.). These points were manually reclassified as default. Ground surface rasters were then developed from triangulated irregular networks (TINs) of ground points.

3.4 Contour Development

Contour lines were derived at 2 foot intervals from ground-classified LiDAR point data using TerraSolid processing software in MicroStation v. 9.01. Contour generation from LiDAR point data requires a smoothing and thinning operation in order to reduce contour sinuosity. Parameters for these operations are: smoothing elevation bounds +/- 0.2 feet; thinning elevation bounds: +/- 0.2 feet; search radius 20 feet. The thinning operation reduces point density where topographic change is minimal (flat surfaces) while preserving resolution where topographic change is present. The total sum of potential error in vertical position is equal to twice the point processing limits (0.40 feet) plus twice the 2-sigma absolute vertical accuracy value for this dataset.

Ground point density rasters were created within MicroStation using a 3-foot step resolution and a 6-foot sampling radius. Areas with less than 0.02 ground-classified points per square foot were considered “sparse” and areas with higher densities were considered “covered”. The ground point density raster data are in ESRI GRID format and have a 3-foot pixel resolution. The contour lines were intersected with ground point density raster data, allowing the addition of a confidence attribute to contour lines. Contour lines over “sparse” areas have low confidence, while contour lines over “covered” areas have a high confidence. Areas with low ground point density are commonly beneath buildings and bridges, in locations with dense vegetation, over water, and in other areas where laser penetration to the ground surface is impeded. **Figure 3** is an example of a ground point density raster and contour lines and **Figure 4** displays high and low confidence contours as green and red, respectively.

Figure 3. Elevation contours over LiDAR ground-classified point density raster (left) and true-color aerial photograph (right). Red indicates low ground point density and blue represents high density.

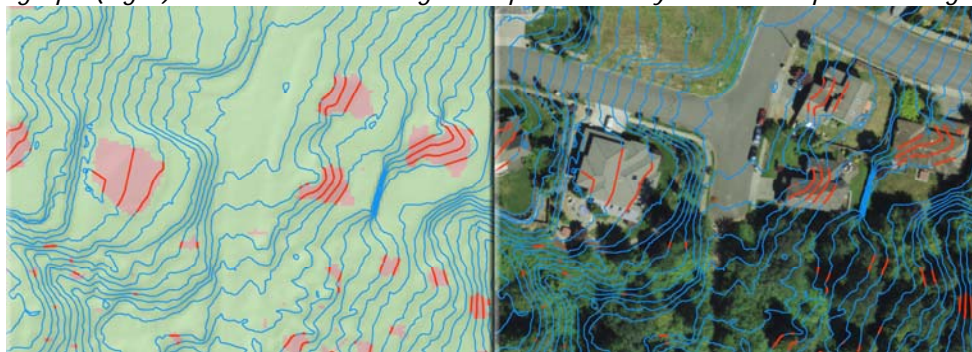
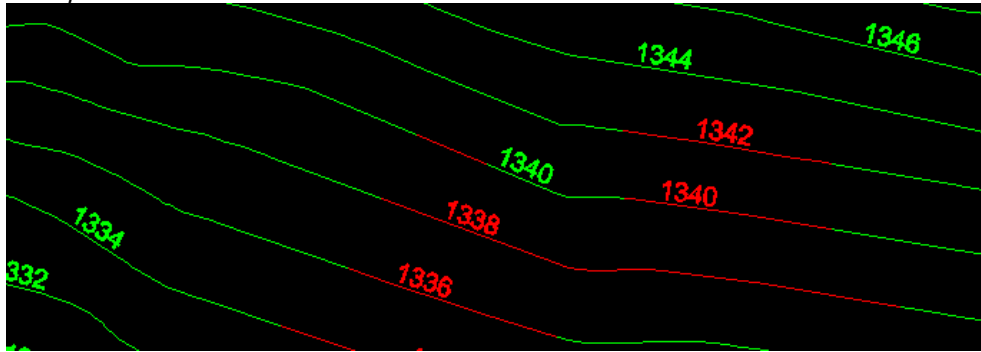


Figure 4. Example of elevation contours in CAD format.



4. LiDAR Accuracy Assessment

4.1 Laser Noise and Relative Accuracy

Laser point absolute accuracy is largely a function of laser noise and relative accuracy. To minimize these contributions to absolute error, we first performed a number of noise filtering and calibration procedures prior to evaluating absolute accuracy.

Laser Noise

For any given target, laser noise is the breadth of the data cloud per laser return (i.e., last, first, etc.). Lower intensity surfaces (roads, rooftops, still/calm water) experience higher laser noise. The laser noise range for this survey was approximately 0.02 meters.

Relative Accuracy

Relative accuracy refers to the internal consistency of the data set - the ability to place a laser point in the same location over multiple flight lines, GPS conditions, and aircraft attitudes. Affected by system attitude offsets, scale, and GPS/IMU drift, internal consistency is measured as the divergence between points from different flight lines within an overlapping area. Divergence is most apparent when flight lines are opposing. When the LiDAR system is well calibrated, the line-to-line divergence is low (<10 cm). See Appendix A for further information on sources of error and operational measures that can be taken to improve relative accuracy.

Relative Accuracy Calibration Methodology

1. **Manual System Calibration:** Calibration procedures for each mission require solving geometric relationships that relate measured swath-to-swath deviations to misalignments of system attitude parameters. Corrected scale, pitch, roll and heading offsets were calculated and applied to resolve misalignments. The raw divergence between lines was computed after the manual calibration was completed and reported for each survey area.
2. **Automated Attitude Calibration:** All data were tested and calibrated using TerraMatch automated sampling routines. Ground points were classified for each individual flight line and used for line-to-line testing. System misalignment offsets (pitch, roll and heading) and scale were solved for each individual mission and applied to respective

mission datasets. The data from each mission were then blended when imported together to form the entire area of interest.

3. **Automated Z Calibration:** Ground points per line were used to calculate the vertical divergence between lines caused by vertical GPS drift. Automated Z calibration was the final step employed for relative accuracy calibration.

4.2 Absolute Accuracy

Laser point absolute accuracy is largely a function of laser noise and relative accuracy. To minimize these contributions to absolute error, a number of noise filtering and calibration procedures were performed prior to evaluating absolute accuracy. The LiDAR quality assurance process uses the data from the real-time kinematic (RTK) ground survey conducted in the AOI. For this project a total of **352 RTK GPS** measurements were collected on hard surfaces distributed among multiple flight swaths. To assess absolute accuracy the location coordinates of these known RTK ground points were compared to those calculated for the closest ground-classified laser points.

The vertical accuracy of the LiDAR data is described as the mean and standard deviation (sigma - σ) of divergence of LiDAR point coordinates from RTK ground survey point coordinates. To provide a sense of the model predictive power of the dataset, the root mean square error (RMSE) for vertical accuracy is also provided. These statistics assume the error distributions for x, y, and z are normally distributed, thus the skew and kurtosis of distributions are also considered when evaluating error statistics.

Statements of statistical accuracy apply to fixed terrestrial surfaces only and may not be applied to areas of dense vegetation or steep terrain (See Appendix A).

5. Study Area Results

Summary statistics for point resolution and accuracy (relative and absolute) of the LiDAR data collected in the Broadwater, MT survey area are presented below in terms of central tendency, variation around the mean, and the spatial distribution of the data (for point resolution by tile).

5.1 Data Summary

Table 2. LiDAR Resolution and Accuracy - Specifications and Achieved Values

	Targeted	Achieved
Resolution:	≥ 8 points/m ²	8.21 points/m ² (.766 points/foot ²)
*Vertical Accuracy (1 σ):	<15 cm	1.9 cm

5.2 Data Density/Resolution

The average first-return density of delivered dataset is 8.21 points per square meter (Table 2). The initial dataset, acquired to be ≥ 8 points per square meter, was filtered as described previously to remove spurious or inaccurate points. Additionally, some types of surfaces (i.e., dense vegetation, breaks in terrain, water, steep slopes) may return fewer pulses (delivered density) than the laser originally emitted (native density).

Ground classifications were derived from automated ground surface modeling and manual, supervised classifications where it was determined that the automated model had failed. Ground return densities will be lower in areas of dense vegetation, water, or buildings.

Figures 7 and 8 show the distribution of average native and ground point densities for each processing bin.

Cumulative LiDAR data resolution for the Broadwater, MT AOI:

- Average Point (First Return) Density = .766 points/foot² (8.21 points/m²)
- Average Ground Point Density = .361 points/foot² (3.88 points/m²)

Figure 5. Density distribution for first return laser points

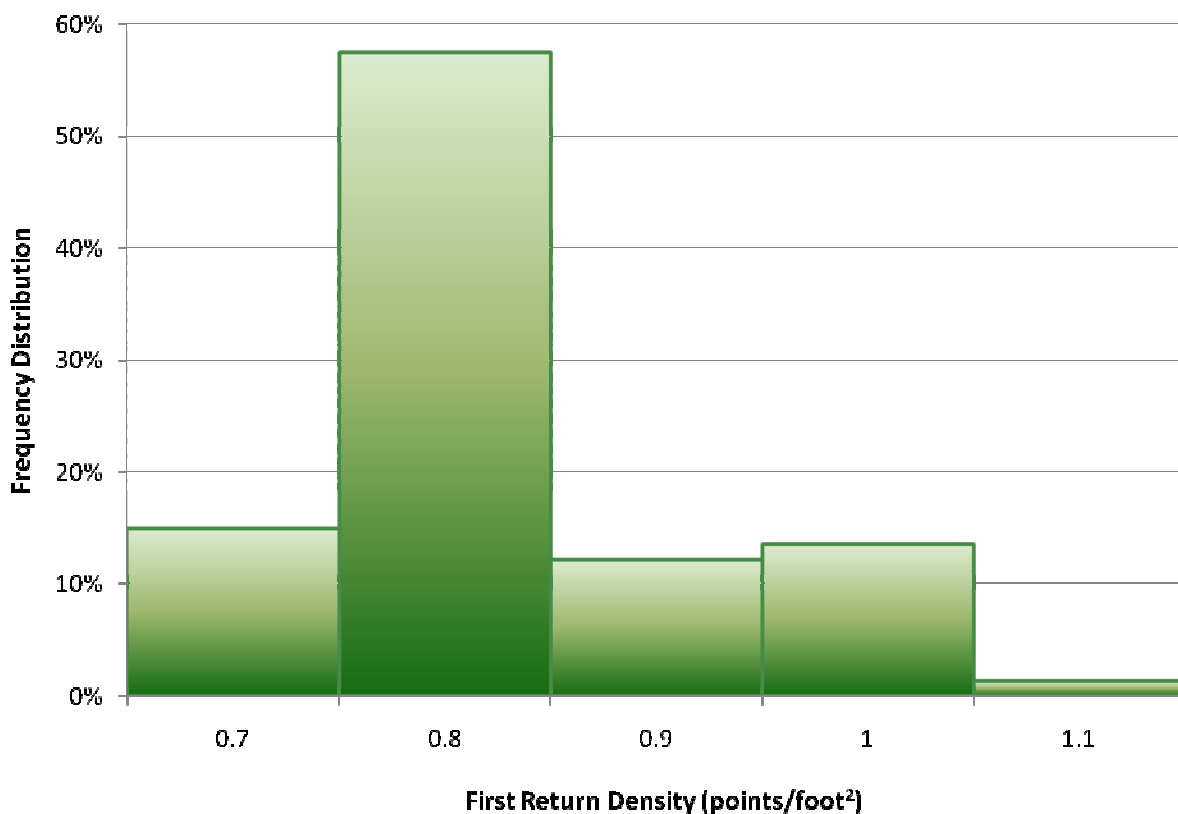


Figure 6. Density distribution for ground classified laser points

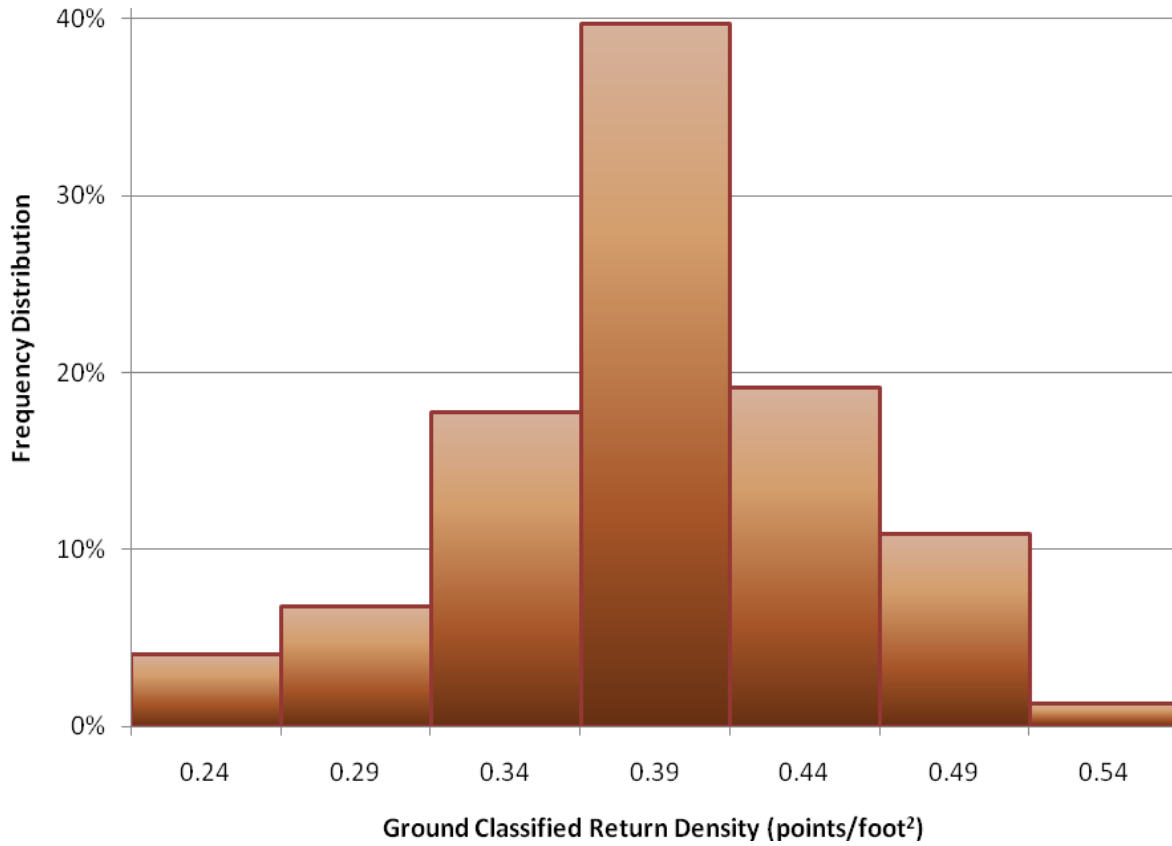


Figure 7. Density distribution map for first return points by processing bin

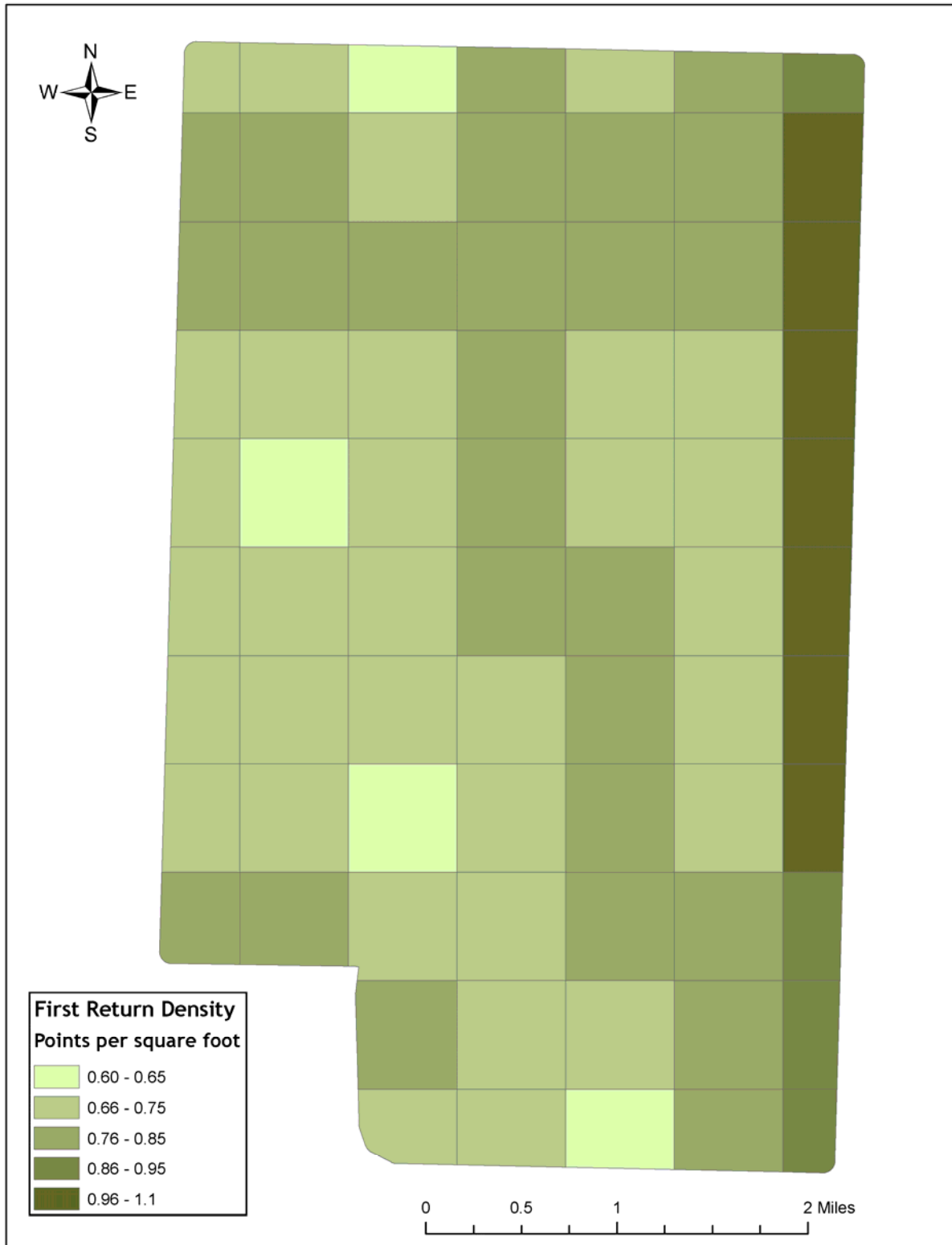
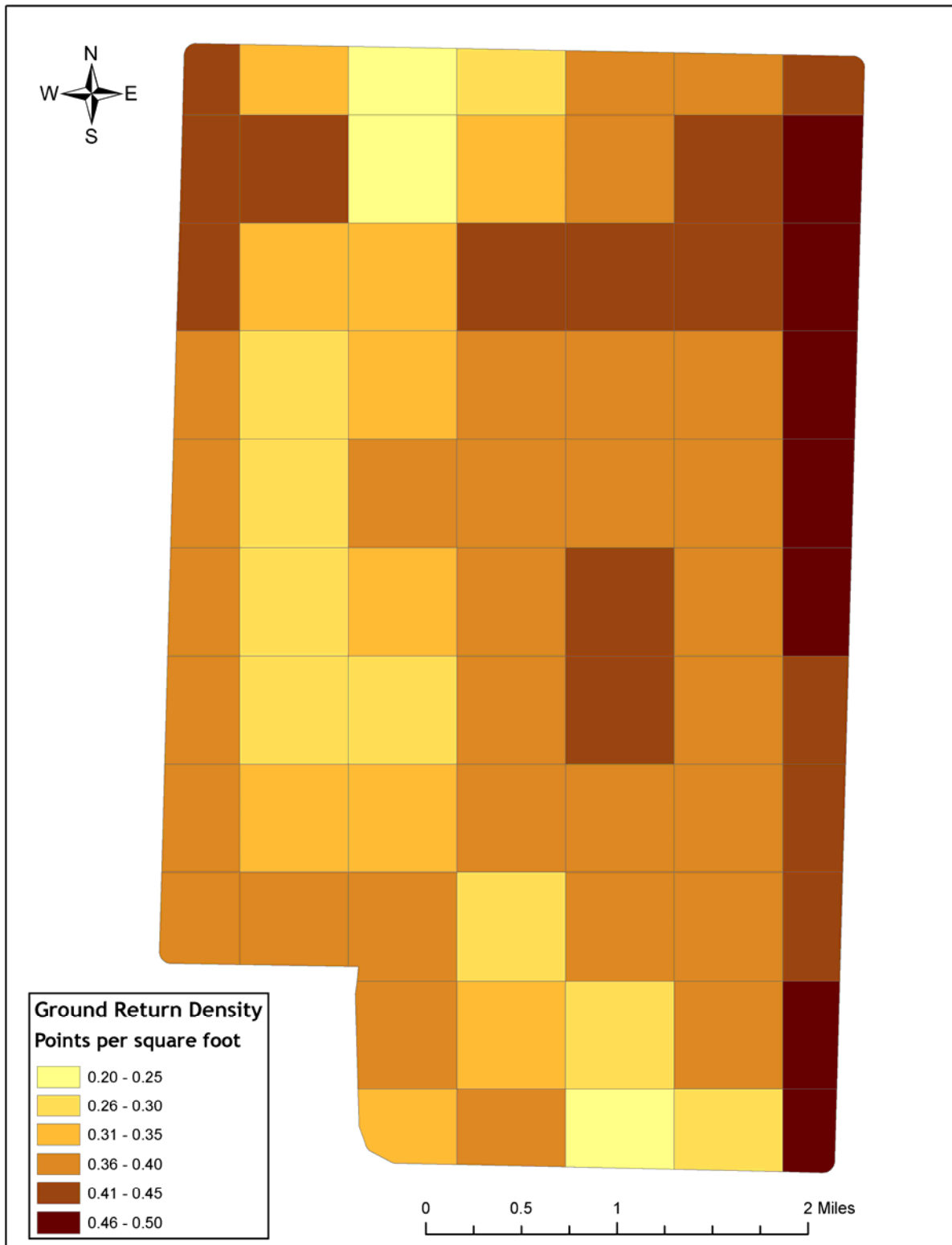


Figure 8. Density distribution map for ground return points by processing bin

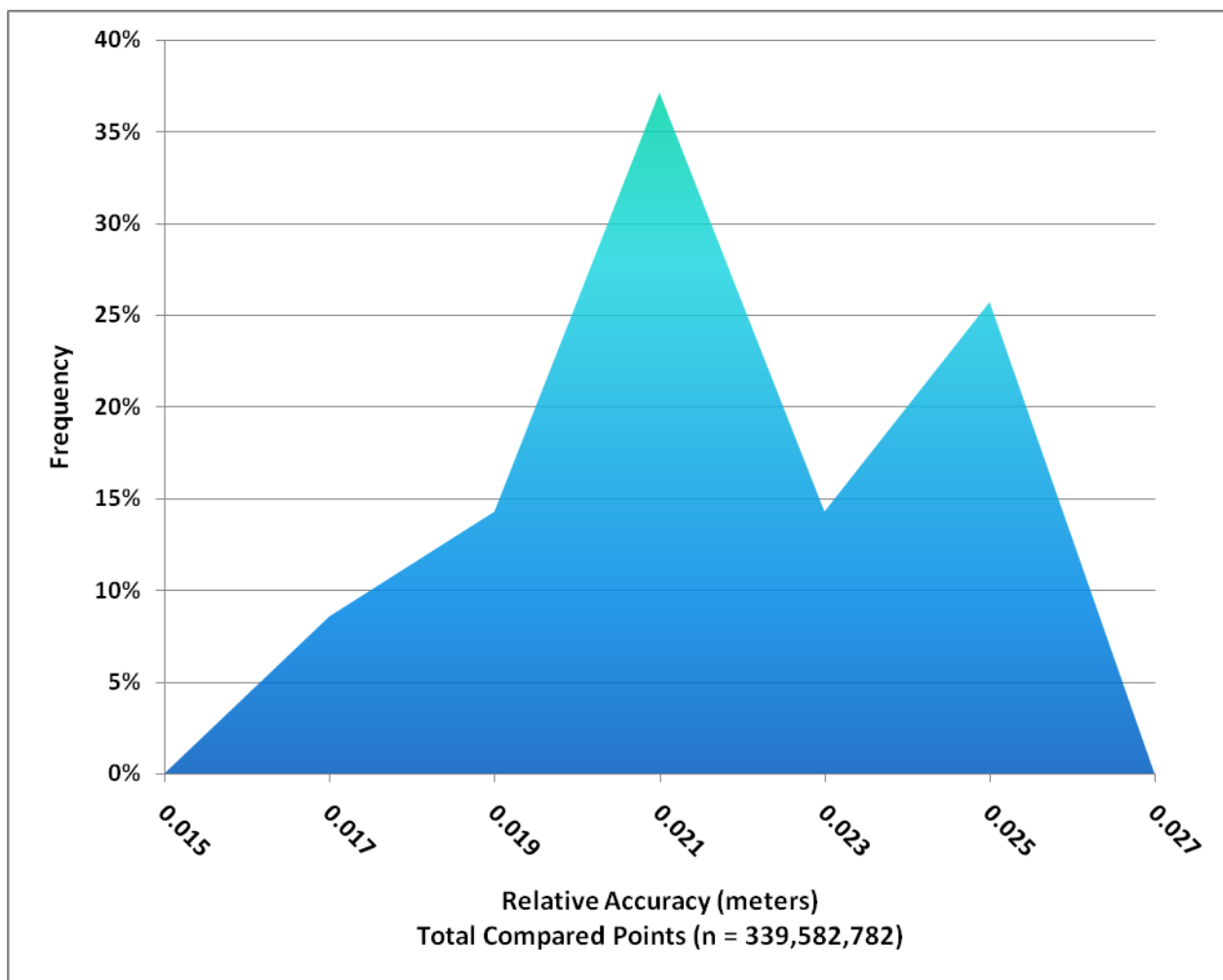


5.3 Relative Accuracy Calibration Results

Relative accuracy statistics for the Broadwater, MT dataset measure the full survey calibration including areas outside the delivered boundary:

- Project Average = 0.020 m (.067 ft)
- Median Relative Accuracy = 0.020m (.066 ft)
- 1 σ Relative Accuracy = 0.003m (.008 ft)
- 1.96 σ Relative Accuracy = 0.005m (.016 ft)

Figure 9. Distribution of relative accuracies per flight line, non slope-adjusted



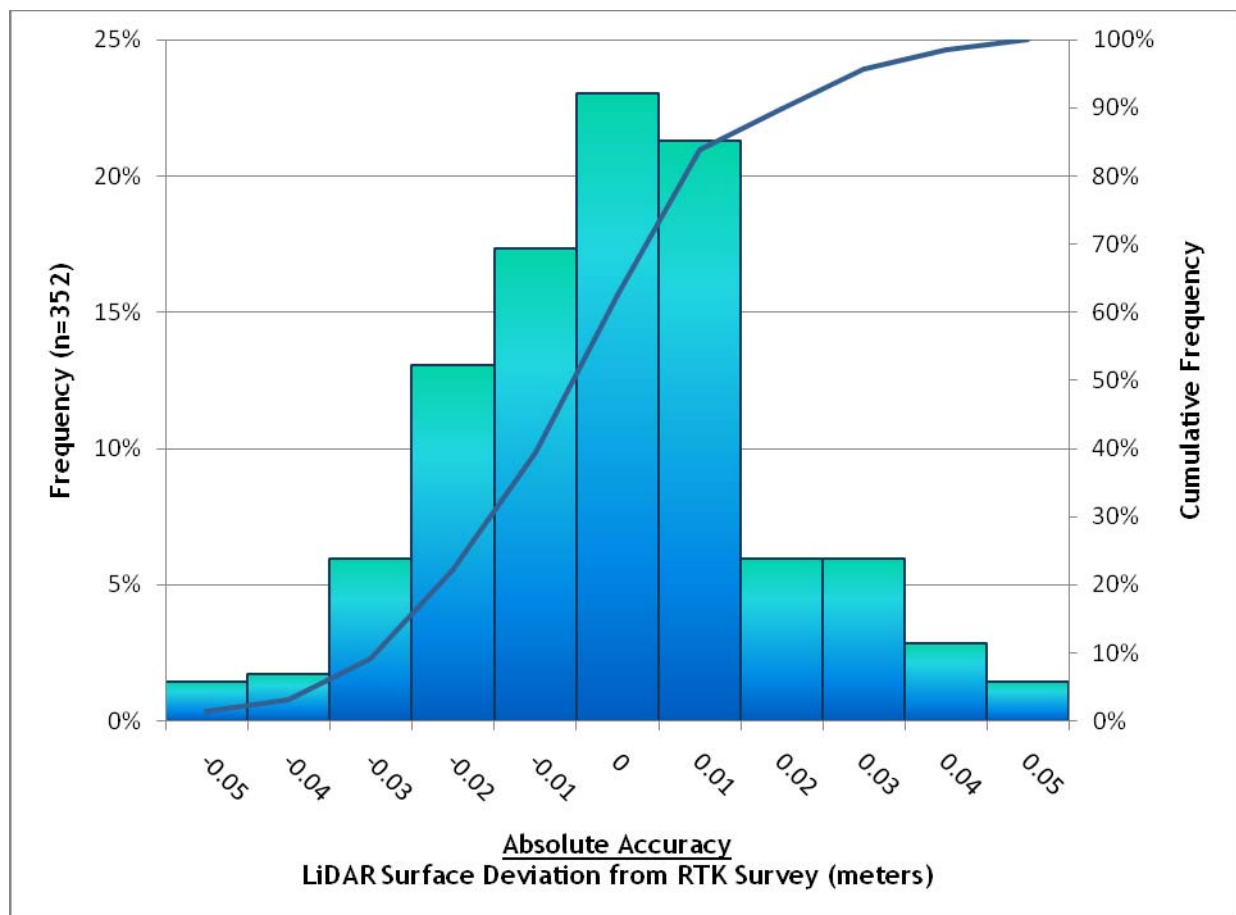
5.4 Absolute Accuracy

Absolute accuracies for the Broadwater, MT survey area:

Table 3. Absolute Accuracy - Deviation between laser points and RTK hard surface survey points

RTK Survey Sample Size (n): 352	
Root Mean Square Error (RMSE) = 0.020m (.066 ft)	Minimum Δz = -0.055m (-.180 ft)
Standard Deviations 1 sigma (σ): 0.019m (.062 ft) 1.96 sigma (σ): 0.037m (.111 ft)	Maximum Δz = 0.048m (.157 ft)
	Average Δz = -0.005m (-.016ft)

Figure 10. Absolute Accuracy - Histogram Statistics



5.5 Accuracy per Land Cover

In addition to the hard surface RTK data collection, points were also collected independently on five different land cover types within in the Broadwater AOI by Professional Consultants, Inc. (MT Professional Licensed Surveyor, Roger Austin). (Figure 11) In accordance with FEMA Standards for LiDAR and Digital Topographic Mapping, individual accuracies were calculated for each land-cover type to assess confidence in the LiDAR derived ground models across land-cover classes. Accuracy statistics for each land cover class are reported in Table 4.

The land cover classes for Broadwater, MT study area include:

- Gravel**
- Pavement**
- Short Vegetation
- Shrubs
- Tall Grass

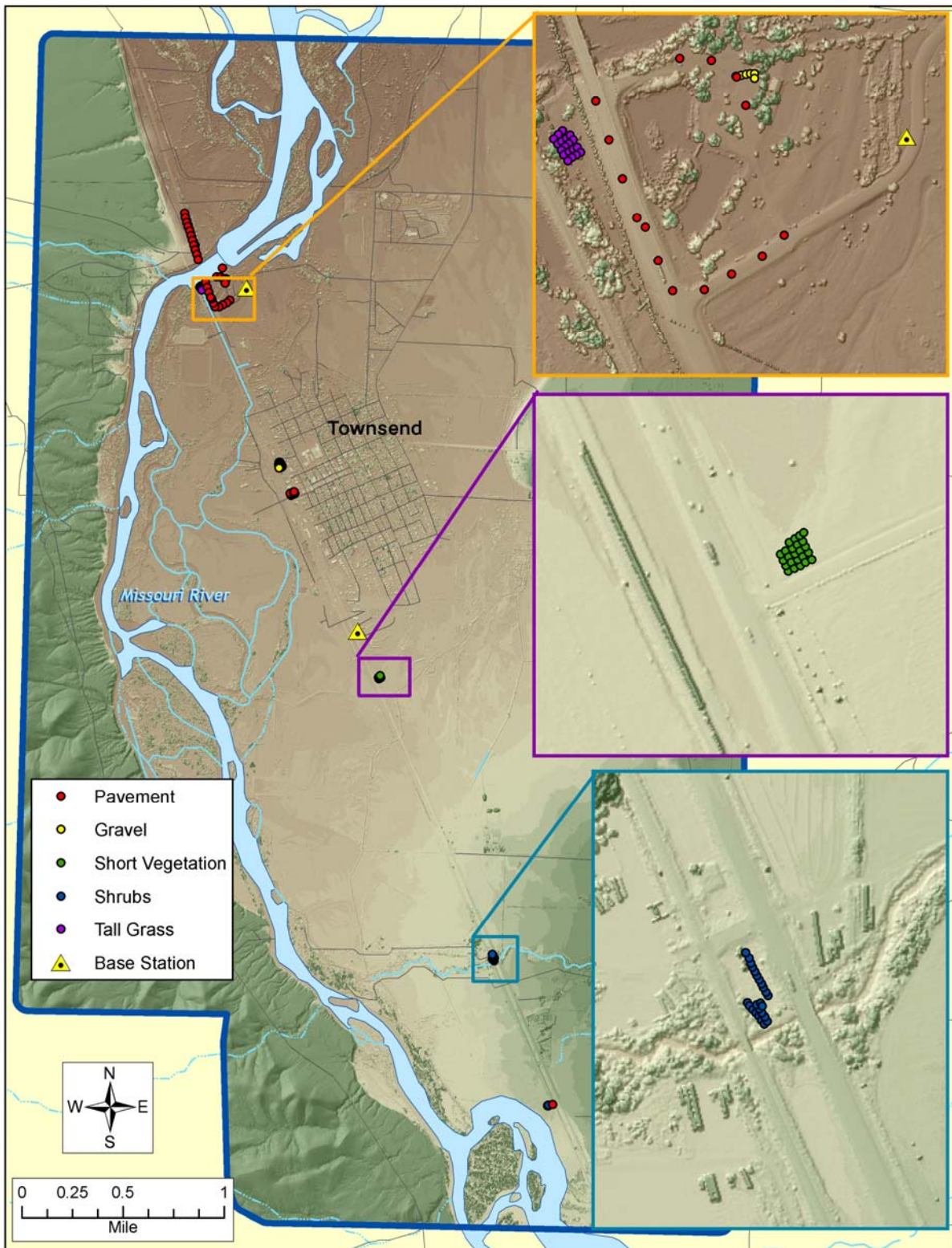
**Four check points were identified as outliers within the dataset due to inconsistency with adjacent points: *pavement points 502, 503, & 540 and gravel point 103*. Three additional check points had no land cover class and were also excluded - 297, 362, & 376. Summary statistics were calculated with and without these points (Table 4).

Table 4. Summary of absolute accuracy statistics for each land cover type

Land cover	Sample size (n)	Mean Dz : feet	1 sigma (σ): feet	1.96 sigma (σ): feet	RMSE: feet
Gravel	46	-.055	.068	.133	.087
<i>Gravel*</i>	47	-.049	.078	.153	.092
Pavement	73	.020	.061	.120	.064
<i>Pavement*</i>	76	.011	.112	.220	.112
Short Vegetation	24	-.024	.085	.167	.087
Shrubs	30	.274	.227	.445	.354
Tall Grass	19	.253	.116	.227	.277

**outliers included in summary statistics*

Figure 11. Land cover RTK check point locations



6. Bathymetric Survey

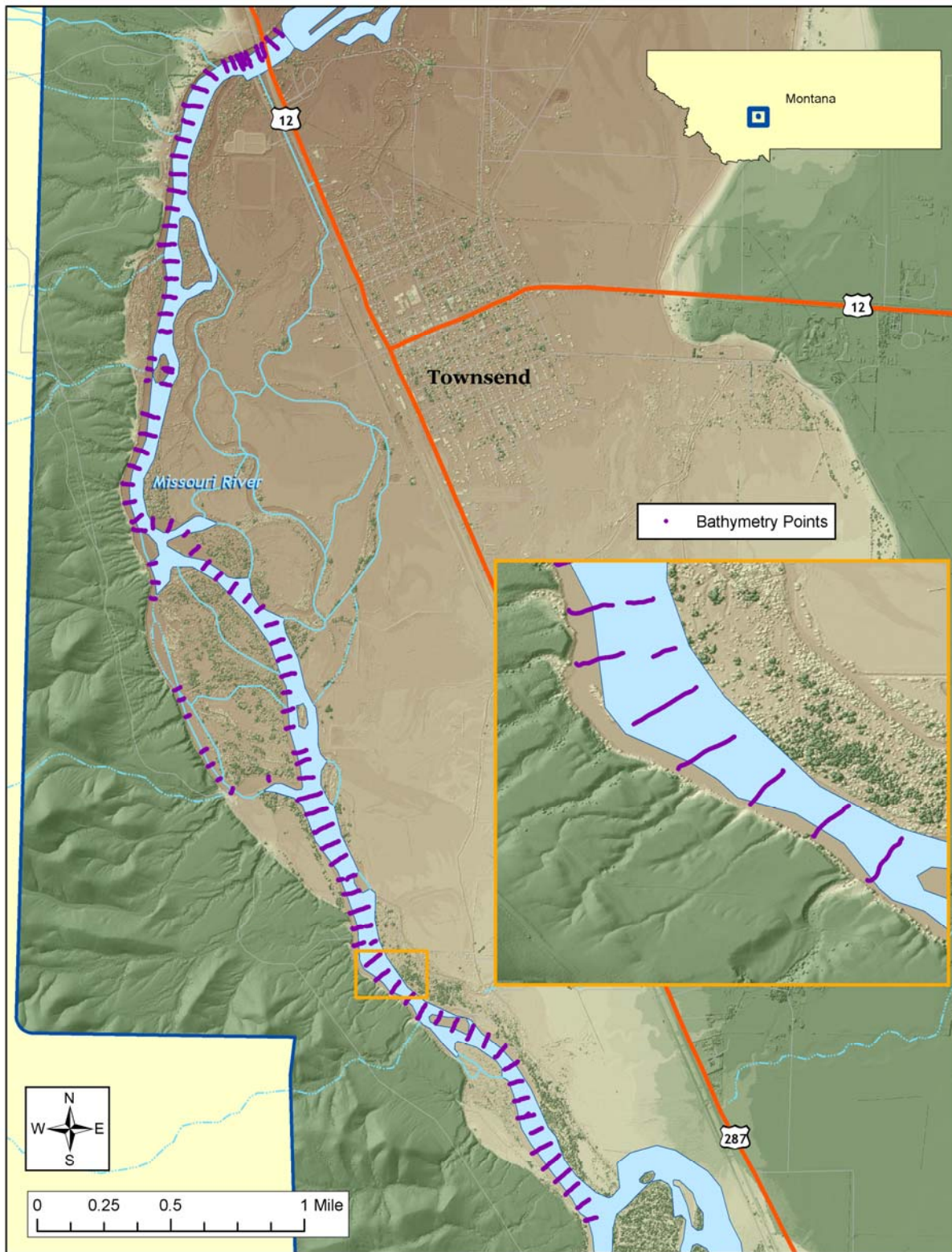
6.1 Overview

A bathymetric survey was conducted along 5.5 river miles of the Missouri River (including accessible backchannels) in the Broadwater LiDAR survey area using hydro-acoustic technology. Since the airborne LiDAR does not penetrate water surface, hydro-acoustic data were collected to provide a continuous terrain surface model to support hydraulic and engineering analysis in the study reaches. The bathymetry data were collected from November 17th- 19th by Solmar Hydro Inc. based in Portland, OR. This data set provides a spatially continuous complement to the high resolution LiDAR data. The two datasets were integrated by Watershed Sciences to produce a seamless combined elevation model. This section provides a detailed overview of the collection and processing of the hydro-acoustic data.

The bathymetric data were collected in cross-sectional transects spaced ~350ft apart depending on the study reach. Additional bathymetric cross-sections were taken around the Route 12 Bridge. **Figure 12** illustrates the distribution of bathymetric data collected.

The bathymetric data were collected on a subset of the total LiDAR area.

Figure 12. Distribution of bathymetric data points (displayed over highest hit model)



6.2 Bathymetric Survey - Instrumentation and Methods

Bathymetric data were collected using an Odom CV100 echosounder system with a 4°, 200 kHz transducer. Positioning and time stamp information was provided by a Trimble R8 GNSS GPS (GLONAS enabled) with the signal being routed into the Odom CV100 echosounder and coupled in real-time with the hydroacoustic data in HYPACK v2009a. The Trimble R8 GPS also provides realtime navigation information which was fed into an onboard computer and overlaid onto pre-



Figure 13 - Survey Vessel used for the Missouri River Bathymetric Survey. The Trimble R8 antenna is located on top of the red sonar mast.

mapped transects. The survey vessel was an 18-foot Duckworth Sled powered by a 130 hp Suzuki Jet pump (Figure 13). The transducer was mounted to the side of the vessel below the Trimble GPS and submerged to a depth of 1.1ft.

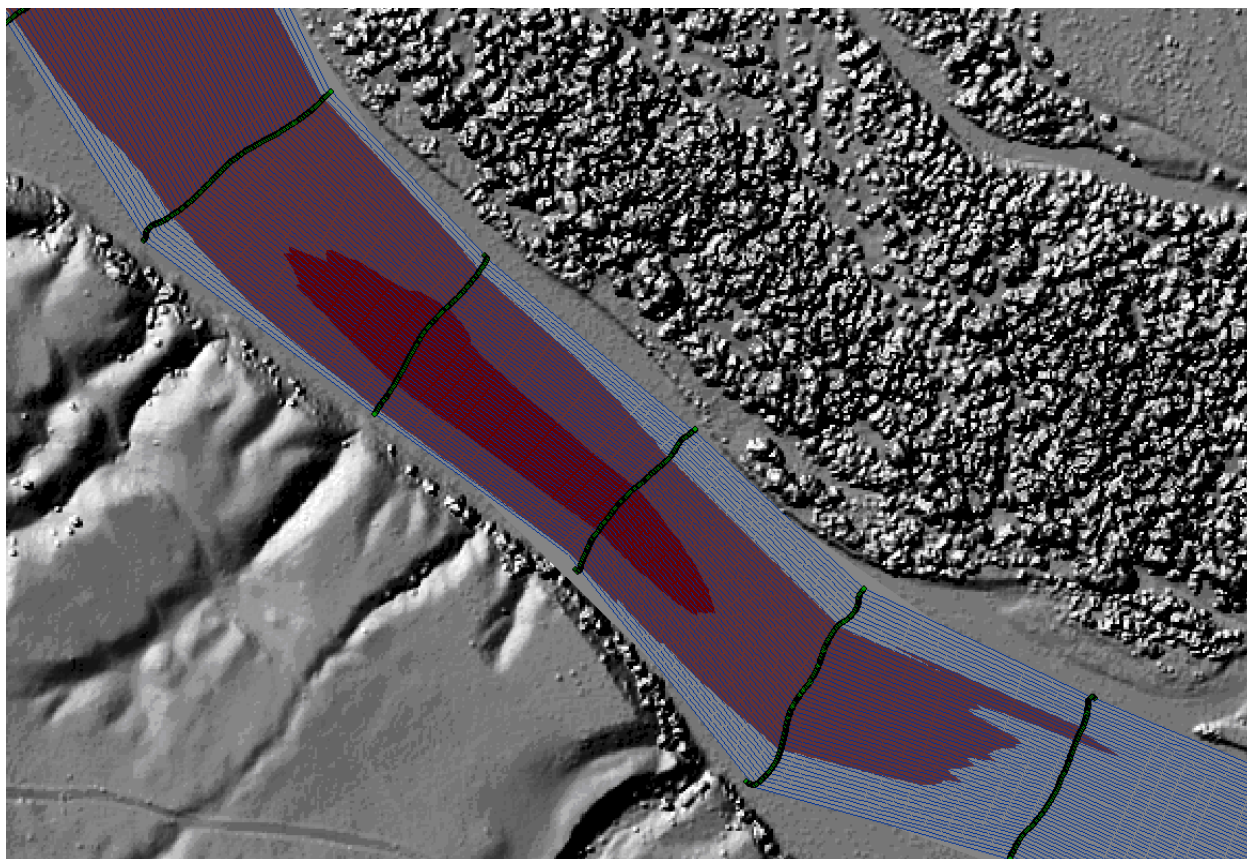
During the hydroacoustic survey a Trimble R-8 was set up over monument #RW0582, the same survey monuments used during the LiDAR survey (Table 1). In order to obtain accurate vertical positions, a Trimble R8 GPS antenna was mounted directly over the transducer and configured to record RTK data at a 5-Hz interval. HDOP was monitored throughout the survey and did not exceed 2.5.

6.3 Bathymetric Data Processing

Bathymetric data were processed using HYPACK v2009a with depth measurements being recorded at 15 Hz. The minimum depth sounding per foot along each transect was considered bottom location. All data files were extensively reviewed for spurious soundings from aquatic vegetation or noise due to aeration in the water column. The SONAR data was then joined with the GPS files based on the time stamp. A straight line interpolation was used to fill in the difference in data densities of the two data sets (15 Hz -SONAR, 5 Hz - GPS). A latency test was performed to determine delay time between the GPS and echosounder. Timing delays in the system were determined by running reciprocal survey lines over a changing bottom. HYPACK then varies the time delay of the test survey to determine the “best fit” setting. For this survey a latency of 0.15 seconds was applied.

Bathymetric elevations along each cross-section were derived by associating the hydroacoustic depth with the GPS position via GPS timestamp. Bottom surface positions and elevations were then calculated by subtracting the depth measurement from GPS position. Raw bathymetric positions were then spatially summarized in ArcGIS for development of an interpolated bathymetric surface model (Figure 14).

Figure 14. 2-D image of linear interpolation between cross-sections overlaid on LiDAR-derived highest-hit hillshade of Broadwater Survey Site.



6.4 Bathymetric Accuracy Assessment

Accuracy of the final bathymetric model can best be understood in terms of component accuracies including: **1)** positional accuracy of sonar/transducer; **2)** timing differences between the GPS and sonar; **3)** boat attitude at the time of sounding (i.e. pitch, roll, yaw); **4)** instrumentation tolerances; and **5)** interpolation error.

Positional accuracy of the sonar/transducer (**#1**) was discussed previously (Section 6.2 - 6.3) and after post-processing, is not considered a significant source of error. Timing difference between the GPS and sonar (**#2**) was measured and corrected for using a calibration transect (or latency test) at the beginning of the survey. The boat attitude (**#3**) was not measured and therefore could not be quantified. However, the river surface conditions and boat configuration were relatively constant throughout the survey and this error was considered relatively minor. The accuracy of the CV100 echosounder (**#4**) is ± 0.1 ft, and the minimum sounding depth was ~ 2 ft.

Several independent checks were performed with a leveling rod to verify hydro-acoustically derived elevations along transects. Digitized soundings were within 0.2ft of elevation checks

measured with the leveling rod, indicating a high degree of accuracy in the hydroacoustic transect data.

The most significant source of potential error is interpolation (#5), both between distant cross-sections and between the hydro acoustically derived bathymetric surface and the LiDAR derived bank elevations. Interpolation error is unavoidable with transect based hydrographic surveys and steps were taken to minimize this in the development of the bathymetric and combined elevation models.

7. Combined Elevation Model

Integration of the hydroacoustic data with the LiDAR data was a five step process.

- 1) Create an interpolated bathymetry surface of the main channel using linear interpolation between main-channel transects.
Software: ArcGIS 9.3.1
- 2) Warp interpolated main-channel surface to fit stream features (i.e. bends, islands, narrows).
Software: ArcGIS 9.3.1
- 3) Generate regular points within main channel and assign elevations from warped interpolated bathymetry surface.
Software: ArcGIS v.9.3.1
- 4) Extract ground model-key points from terrestrial LiDAR using digitized water and island masks.
Software: MicroStation v.8, TerraScan v.9.001, ArcGIS v.9.3.1
- 5) Combine main-channel points, LiDAR ground returns, breakpoints, and back-channel depth points into a single elevation model.
Software: Microstation v.8, ArcGIS v. 9.3.1
- 6) Manually inspect combined bathymetric mode for interpolation errors removing erroneous features when identified.
Software: Microstation v.8, ArcGIS v. 9.3.1

7.1 Bathymetric Processing

It was necessary to generate the bathymetry model in multiple stages to prevent mis-interpolation between main-channel transects and back-channel or water edge points. First a TIN surface was interpolated from main-channel transects only. This forced the direction of interpolation to follow the river current. Because meander of the river was such that direct linear interpolation between cross-sections did not adequately capture the character of the river, the interpolated surface was warped to better fit the river banks. Additional points were then generated between transects and assigned elevation based on the interpolated main-channel surface. These newly generated points were used to represent the main channel in the final model (**Figures 15 & 16**). Because the new points are more evenly distributed throughout the main channel they create a more accurate bathymetric representation when combined with ground points at the water edge.

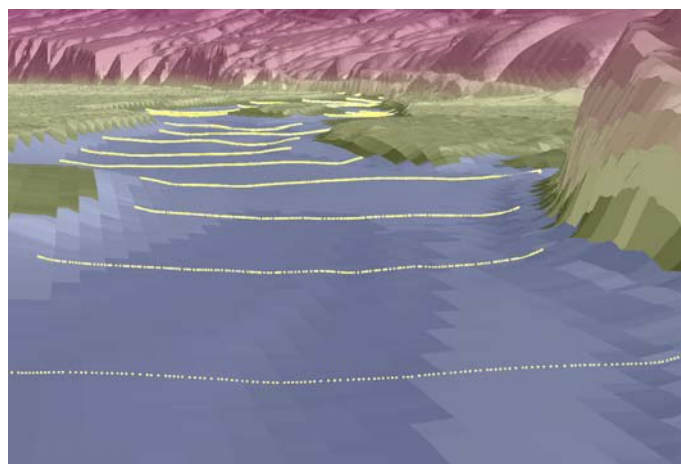


Figure 15 - Hydroacoustic cross sections displayed over the combined LiDAR and bathymetric models for the Broadwater Study Site (vertical exaggeration = 2.0)

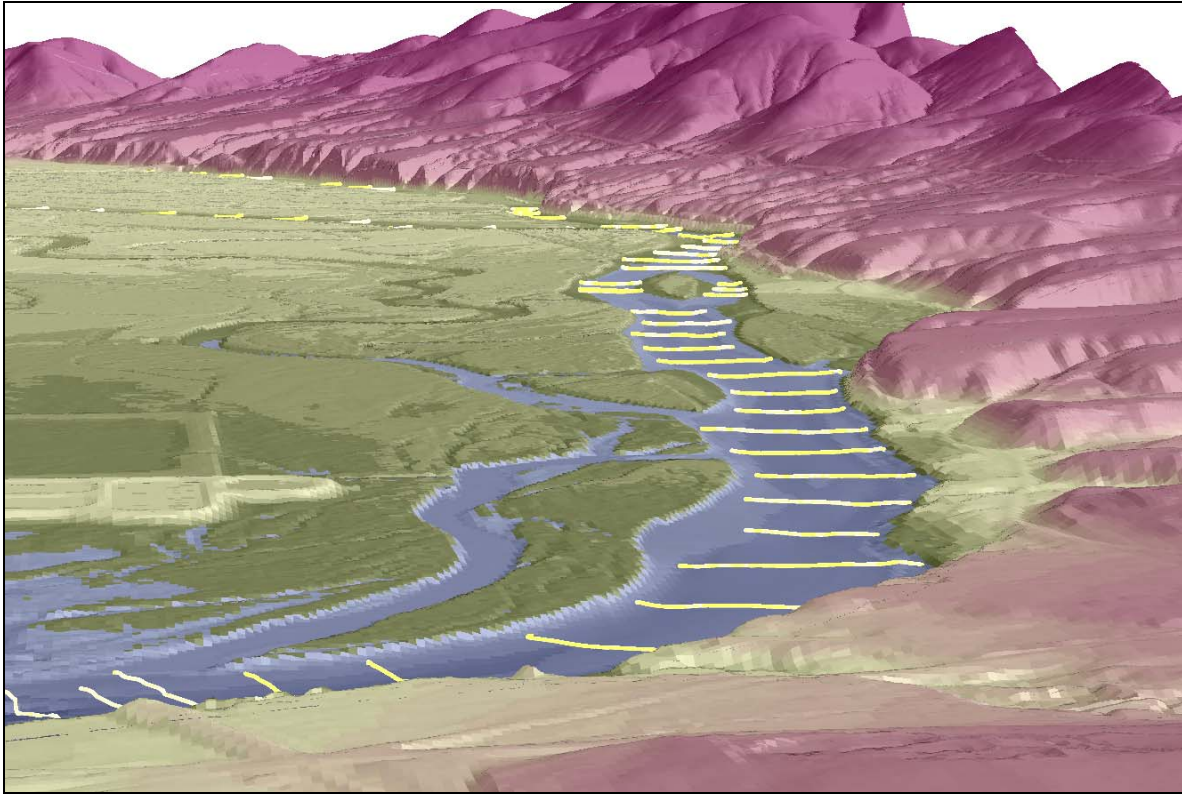
7.2 Terrestrial LiDAR Extraction

Extracting the terrestrial LiDAR data required a water mask digitized using LiDAR intensity images and ground models. Ground classified LiDAR points within the water mask were reclassified to an intermediate class so the bathymetry points could be used to develop a seamless model. A classification routine was run in TerraScan (LiDAR point processing software) to generate a new ground surface from bathymetry points and LiDAR points. The parameters for this routine started with an initial points spacing of 20ft then added or removed ground points as necessary to represent the full density LIDAR ground model within a vertical tolerance of +/- 0.2ft.

7.3 Combined Elevation Model

The final integrated model was developed by combining 1) main-channel and back-channel bathymetry points from the surface interpolated between hydroacoustic cross-sections, 2) model key points extracted from the terrestrial LiDAR data. In Microstation v.8, an integrated surface was interpolated from the combined points generating a seamless representation of both the terrestrial and aquatic bare-earth. (**Figure 16**)

Figure 16. 3D image derived from LiDAR and Bathymetric data overlaid with cross sections looking south along Missouri River



8. Projection/Datum and Units

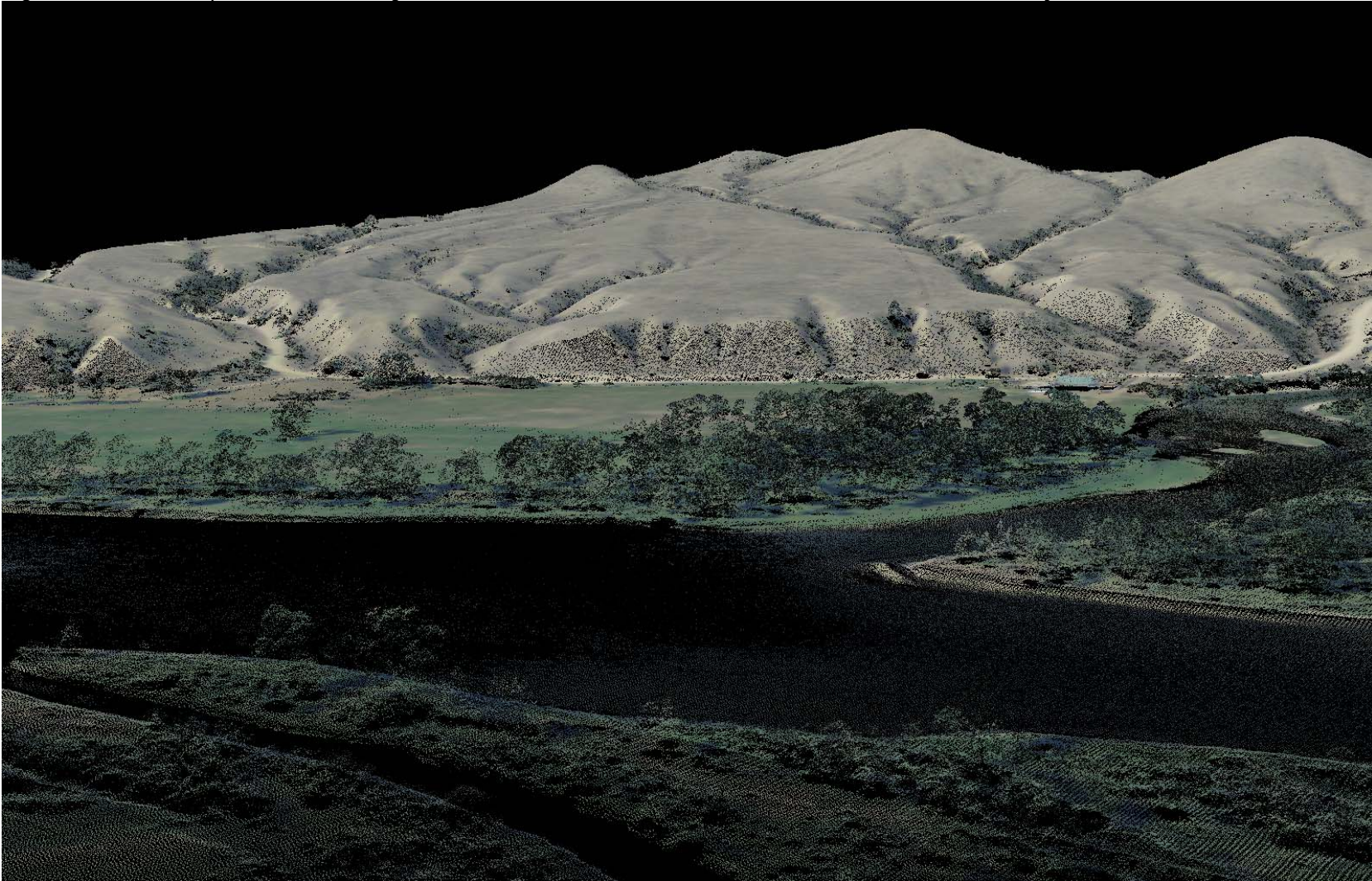
	Projection:	Montana State Plane, NAD 83
Datum	Vertical:	NAVD88 Geoid09
	Horizontal:	NAD83
	Units:	Horizontal - International Feet Vertical - US Feet

9. Deliverables

Point Data:	<ul style="list-style-type: none"> All Returns (LAS 1.2 format)
Vector Data:	<ul style="list-style-type: none"> Tile Index of LiDAR Points (shapefile format) Contours (2 ft - DXF format)
Raster Data:	<ul style="list-style-type: none"> Elevation Models (3 ft resolution) <ul style="list-style-type: none"> Bare Earth Model (ESRI GRID format) Highest Hit Model (ESRI GRID format) Intensity Images (GeoTIFF format, 1.5 ft resolution) Combined Elevation Model (ASCII text format)
Data Report:	<ul style="list-style-type: none"> Full report containing introduction, methodology, and accuracy

10. Selected Images

Figure 17. 3D LiDAR point cloud looking west over the Missouri River, south of Townsend, MT (colored by 2009 NAIP)



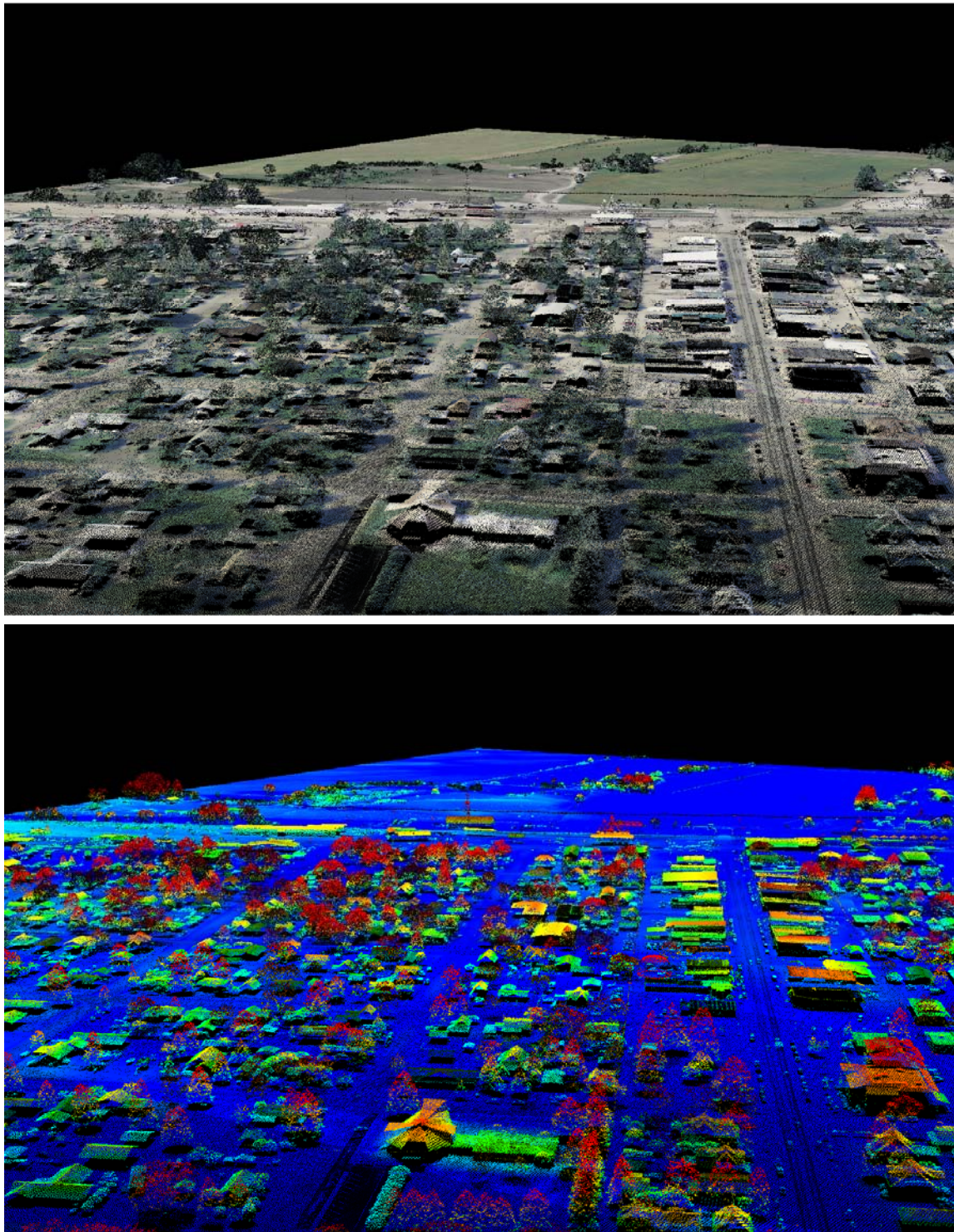
LiDAR Data Acquisition and Processing: Broadwater, MT

Prepared by Watershed Sciences, Inc.

Figure 18. 3D LiDAR point cloud of an island and side channel of the Missouri River (colored by 2009 NAIP)



Figure 19. 3D LiDAR point cloud of residential Townsend, MT (top colored by 2009 NAIP, bottom colored by elevation)



11. Glossary

1-sigma (σ) Absolute Deviation: Value for which the data are within one standard deviation (approximately 68th percentile) of a normally distributed data set.

1.96-sigma (σ) Absolute Deviation: Value for which the data are within two standard deviations (approximately 95th percentile) of a normally distributed data set.

Root Mean Square Error (RMSE): A statistic used to approximate the difference between real-world points and the LiDAR points. It is calculated by squaring all the values, then taking the average of the squares and taking the square root of the average.

Pulse Rate (PR): The rate at which laser pulses are emitted from the sensor; typically measured as thousands of pulses per second (kHz).

Pulse Returns: For every laser pulse emitted, the Leica ALS 50 Phase II system can record *up to four* wave forms reflected back to the sensor. Portions of the wave form that return earliest are the highest element in multi-tiered surfaces such as vegetation. Portions of the wave form that return last are the lowest element in multi-tiered surfaces.

Accuracy: The statistical comparison between known (surveyed) points and laser points. Typically measured as the standard deviation (σ) and root mean square error (RMSE).

Intensity Values: The peak power ratio of the laser return to the emitted laser. It is a function of surface reflectivity.

Data Density: A common measure of LiDAR resolution, measured as points per square meter.

Spot Spacing: Also a measure of LiDAR resolution, measured as the average distance between laser points.

Nadir: A single point or locus of points on the surface of the earth directly below a sensor as it progresses along its flight line.

Scan Angle: The angle from nadir to the edge of the scan, measured in degrees. Laser point accuracy typically decreases as scan angles increase.

Overlap: The area shared between flight lines, typically measured in percents; 100% overlap is essential to ensure complete coverage and reduce laser shadows.

DTM / DEM: These often-interchanged terms refer to models made from laser points. The digital elevation model (DEM) refers to all surfaces, including bare ground and vegetation, while the digital terrain model (DTM) refers only to those points classified as ground.

Real-Time Kinematic (RTK) Survey: GPS surveying is conducted with a GPS base station deployed over a known monument with a radio connection to a GPS rover. Both the base station and rover receive differential GPS data and the baseline correction is solved between the two. This type of ground survey is accurate to 1.5 cm or less.

12. Citations

Soininen, A. 2004. TerraScan User's Guide. TerraSolid.

Appendix A

LiDAR accuracy error sources and solutions:

Type of Error	Source	Post Processing Solution
GPS (Static/Kinematic)	Long Base Lines	None
	Poor Satellite Constellation	None
	Poor Antenna Visibility	Reduce Visibility Mask
Relative Accuracy	Poor System Calibration	Recalibrate IMU and sensor offsets/settings
	Inaccurate System	None
Laser Noise	Poor Laser Timing	None
	Poor Laser Reception	None
	Poor Laser Power	None
	Irregular Laser Shape	None

Operational measures taken to improve relative accuracy:

1. Low Flight Altitude: Terrain following is employed to maintain a constant above ground level (AGL). Laser horizontal errors are a function of flight altitude above ground (i.e., $\sim 1/3000^{\text{th}}$ AGL flight altitude).
2. Focus Laser Power at narrow beam footprint: A laser return must be received by the system above a power threshold to accurately record a measurement. The strength of the laser return is a function of laser emission power, laser footprint, flight altitude and the reflectivity of the target. While surface reflectivity cannot be controlled, laser power can be increased and low flight altitudes can be maintained.
3. Reduced Scan Angle: Edge-of-scan data can become inaccurate. The scan angle was reduced to a maximum of $\pm 15^\circ$ from nadir, creating a narrow swath width and greatly reducing laser shadows from trees and buildings.
4. Quality GPS: Flights took place during optimal GPS conditions (e.g., 6 or more satellites and PDOP [Position Dilution of Precision] less than 3.0). Before each flight, the PDOP was determined for the survey day. During all flight times, a dual frequency DGPS base station recording at 1-second epochs was utilized and a maximum baseline length between the aircraft and the control points was less than 19 km (11.5 miles) at all times.
5. Ground Survey: Ground survey point accuracy (i.e. <1.5 cm RMSE) occurs during optimal PDOP ranges and targets a minimal baseline distance of 4 miles between GPS rover and base. Robust statistics are, in part, a function of sample size (n) and distribution. Ground survey RTK points are distributed to the extent possible throughout multiple flight lines and across the survey area.
6. 50% Side-Lap (100% Overlap): Overlapping areas are optimized for relative accuracy testing. Laser shadowing is minimized to help increase target acquisition from multiple scan angles. Ideally, with a 50% side-lap, the most nadir portion of one flight line coincides with the edge (least nadir) portion of overlapping flight lines. A minimum of 50% side-lap with terrain-followed acquisition prevents data gaps.
7. Opposing Flight Lines: All overlapping flight lines are opposing. Pitch, roll and heading errors are amplified by a factor of two relative to the adjacent flight line(s), making misalignments easier to detect and resolve.